J. Appl. Comput. Mech., 9(2) (2023) 419-429
DOI: 10.22055/jacm.2022.41759.3805

ISSN: 2383-4536
jacm.scu.ac.ir

Shahid Chamran University of Ahvaz

Journal of Applied and Computational Mechanics

Research Paper

Influence of Thermal Radiation on Heat Transfer through a Hollow Block

Igor V. Miroshnichenko[1], Mikhail A. Sheremet[2]

[1] Laboratory of Mathematical Analysis, The Mechanics and Mathematics Department, Tomsk State University, 36, Lenin Avenue, Tomsk, 634050, Russia, Email: miroshnichenko@mail.tsu

[2] Laboratory on Convective Heat and Mass Transfer, The Mechanics and Mathematics Department, Tomsk State University, 36, Lenin Avenue, Tomsk, 634050, Russia, Email: sheremet@math.tsu.ru

Received August 30 2022; Revised September 24 2022; Accepted for publication September 26 2022.
Corresponding author: I.V. Miroshnichenko (miroshnichenko@mail.tsu.ru)

Abstract. Hollow blocks are widely used in construction to reduce the thermal resistance of building walls. The air within the blocks has a low thermal conductivity, which makes it possible to consider such hollow blocks as a good insulating material. This work presents a numerical investigation of the impact of thermal radiation on energy transport and airflow inside a hollow block. The coupled heat transport by free convection, thermal radiation and conduction through the solid walls is taken into account. The finite-difference procedure is applied to work out numerically the control equations of conservation of momentum, energy and mass in both solid walls and air filled enclosure. The main parameters governing the problem are surface emissivity, Rayleigh number and thermal conductivity of solid walls. The influence of these factors on the overall heat transfer through hollow block is presented and investigated. The outcomes show that the low emissivity of the inner walls inside the hollow blocks will significantly help to reduce the energy consumption of buildings.

Keywords: Hollow blocks; numerical simulation; finite difference method; radiation; coupled heat transfer.

1. Introduction

This Guide has been prepared for authors of papers submitted to JACM (Journal of Applied and Computational Mechanics). Prospective authors are invited to submit papers that fit within the scope of the journal. Improving the energy efficiency of buildings is a priority area of building thermal physics. Thermal insulation characteristics of enclosing structures (walls) play an important role. The use of energy efficient building materials results in enormous energy savings. But such materials must undergo numerical and experimental analysis before being used in construction. Hollow blocks (brick, concrete, etc.) are often used in the construction of buildings due to their high thermal resistance. This is primarily due to the low coefficient of thermal conductivity of the air occupying internal voids. Mathematical modeling in this regard can help control the heat transfer processes inside the hollow blocks.

In 2018, the authors of the present research carried out a detailed review of the numerical and experimental results of heat transfer in closed areas [1]. The articles presented in the study have a wide range of engineering applications, including those in the construction industry. However, in this review, there were not so many works devoted to the joint analysis of convective-radiative energy transport in the walls and enclosing structures of buildings. Over the past 15 years, many interesting articles have been published on the modeling of convective energy transport in enclosures [2-8]. As methods for solving the problems under consideration, the authors used the following methods: lattice Boltzmann technique; finite-volume, finite-difference and finite-element procedures. Separately, it is necessary to note the increased number of publications, where the lattice Boltzmann method is used as a solution method [9-12]. Many scientists are developing this method, mainly in Southeast Asia.

It should be noted that for large characteristic dimensions of the solution region and for significant temperature differences, the flow regime can be changed from laminar to transitional or turbulent. When modeling transient modes of convective heat transfer, according to the authors, turbulent models can be used. In order to better resolve the viscous boundary layer when using grid methods, the grid is usually thickened [13-15]. Such a thickening can be carried out, for example, employing the theory of functions of a complex variable.

In the 21st century, several interesting works have been published regarding the modeling of heat transfer in hollow building elements. Thus, conjugate natural convection and infrared radiation inside honeycomb hollow blocks have been investigated by Boukendil et al. [16]. The air flow in voids was considered to be laminar. Isothermal boundary conditions were considered as additional restrictions at the vertical external boundaries, and the horizontal surfaces of the outer walls were thermally insulated. The control volume method was used as a solution method. They have investigated that the influence of thermal conductivity of

Published online: October 06 2022

solid walls on the contribution of each heat transfer modes (convection, conduction, radiation) is significant. At ΔT = 10 K and λ_w = 0.6 W/(m·K) the contribution of convection, conduction and radiation is 15.45%, 52.42% and 32.13%, respectively. At the same time at ΔT = 10 K and λ_w = 1.0 W/(m·K) the contribution of convection, conduction and radiation is 13.36%, 58.82% and 27.82%, respectively. Influence of construction joint thickness and emissivity on heat transfer through double hollow block has been scrutinized by Boukendil et al. [17]. The thickness of the construction joint plays in some cases an essential role in modeling the energy transport regimes. Surfaces of internal walls of hollow blocks are diffuse-gray. The fluid (air) is supported to be Newtonian and the flow is laminar. As a result of the research, it was found that the use of mortar with a thickness of 1 centimeter is optimal in terms of both the connection of hollow blocks and energy efficiency.

Jamal et al. [18] conducted a study of heat transfer through a hollow clay block during sinusoidal heating. The parameters that determine the problem are the walls emissivity, the period of the exciting temperature and the amplitude. They investigated three configurations of hollow bricks (single layer, double layer and triple layer) and examined the impact of the sinusoidal temperature excitation and the surface emissivity of the internal borders on the overall energy transport through the hollow block. A promising way to suppress the thermal convection in the cavities of blocks is the use of partitions made of solid material. For example, Alhazmy [19] used the internal baffles in order to reduce free convection within the enclosures of hollow brick. Baffles were maintained to the upper and low zones of the inner enclosure, dividing it into three parts. As a result of numerical experiments, the authors managed to increase the thermal resistance by 53 percent compared to the case without baffles. In this work, radiative effects are not taken into account because the impact of ribs on thermogravitational energy transport in cavities is a concern in the present analysis. In recent years, a large number of works have been published devoted to the study of convective heat transfer or hydrodynamic in nanofluids in relation to construction and other engineering applications [20–26]. Manjunatha et al. [27] presented a new theoretical tri-hybrid nanofluid model for enhancing the heat transfer. The tri-hybrid nanofluid is formed by suspending three types of nanoparticles with different physical and chemical bonds into a base fluid. They showed that the heat generated due to strong Lorentz force caused the tri-hybrid nanofluid to conduct more heat. The latent thermal energy storage systems have a prominent energy storage role, with multiple applications in buildings. Alazwari et al. [28] investigated the effects of various types of nanomaterials on phase change materials melting process in a thermal energy storage system for solar cooling application. As a result of the research, it was found that adding Cu, Ag, and CuO nanoparticles does not positively impact the phase change materials melting behavior and boosts the total melting time.

When calculating heat transfer phenomenon through a hollow block, it is necessary to take into account all mechanisms of energy transfer, including radiation. However, in order to reduce computational costs, some authors neglect radiation. However, as the works [29, 30] show, such an account is necessary. Kogawa et al. [31] studied convective-radiative energy transport in a rectangular chamber. The purpose of their study was to find out what effect the radiation of a gas (air) has on the overall heat transfer and hydrodynamics. As a result, they showed that the effect of gas radiation is minimal and its contribution to heat transfer is only a few percent. In this regard, it is advisable to use the surface radiation approximation when solving the class of problems under consideration. Zhou et al. [13] investigated numerically joint thermogravitational and radiative energy transport inside a rectangular cavity having semitransparent walls. The k–ε renormalization group model was applied to simulate the turbulent motion in the cavity. The results showed that a translucent baffle is useful in reducing heat loss and obtaining a higher temperature distribution. Moreover, the transmittance of a translucent wall has a great influence on the thermal and hydrodynamic characteristics of the cavity.

The above review of works shows that the numerical study of heat transfer phenomenon in hollow building elements is relevant. The vast majority of work was carried out taking into account laminar conditions inside the voids of the blocks. This is due to the small size of the internal cavities filled with air. In this work, transient and turbulent flow regimes inside voids will be investigated. This is possible when the characteristic dimensions of voids are more than 10 cm and subject to a more significant temperature difference. This study will take into account heat convection, thermal conduction and surface radiation, that are, all the main mechanisms of energy transfer. The major objective of this research is to scrutinize the impact of radiation inside block on energy transport and liquid circulation.

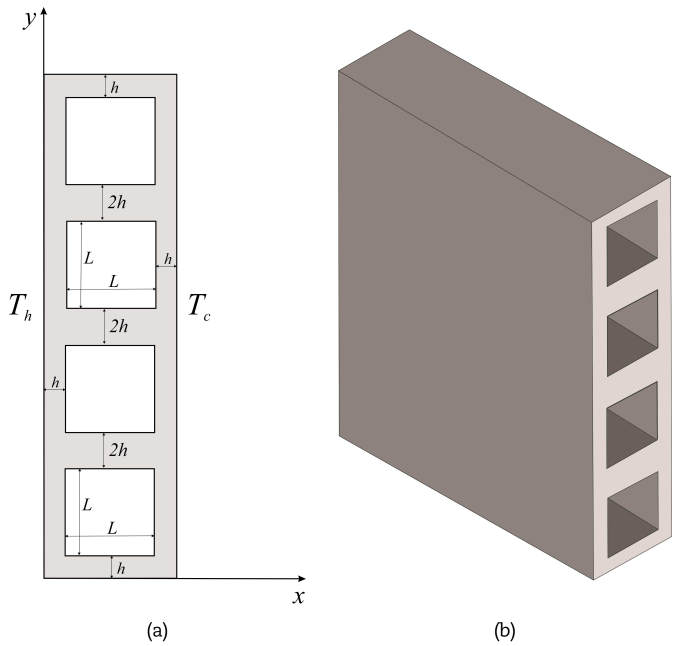

Fig. 1. Schematic diagram of the hollow block (a) and the hollow block (b)

2. Mathematical and Physical Models

The sketch of the analyzed hollow block is demonstrated in Fig. 1*a*. The hollow block includes four square cavities vertically oriented and filled with air having a characteristic size L. The wall thickness between the cavities is 2*h*. The surfaces of the vertical borders of the studied hollow block are assumed to be isothermal and kept at fixed temperatures T_h and T_c, respectively. The horizontal surfaces of external walls are considered adiabatic. The air inside the voids is Newtonian fluid and its physical properties are independent of temperature, with the exception of the density in the buoyancy term, where the Boussinesq approach is employed. The energy transport and airflow is two-dimensional. The air is considered not participating in the radiation, the surfaces inside the voids are considered to be diffuse gray having the same surface emissivity, and the air is considered to be completely transparent. A three-dimensional representation of a hollow building element is shown in Fig. 1*b*.

For two-dimensional heat transfer and unsteady airflow of the presented physical model, the governing equations are:

within the air voids

$$\frac{\partial u}{\partial x}+\frac{\partial v}{\partial y}=0 \tag{1}$$

$$\frac{\partial u}{\partial t}+u\frac{\partial u}{\partial x}+v\frac{\partial u}{\partial y}=-\frac{1}{\rho}\frac{\partial p}{\partial x}+2\frac{\partial}{\partial x}\left[(\nu+\nu_t)\frac{\partial u}{\partial x}\right]+\frac{\partial}{\partial y}\left[(\nu+\nu_t)\left(\frac{\partial u}{\partial y}+\frac{\partial v}{\partial x}\right)\right] \tag{2}$$

$$\frac{\partial v}{\partial t}+u\frac{\partial v}{\partial x}+v\frac{\partial v}{\partial y}=-\frac{1}{\rho}\frac{\partial p}{\partial y}+\frac{\partial}{\partial x}\left[(\nu+\nu_t)\left(\frac{\partial u}{\partial y}+\frac{\partial v}{\partial x}\right)\right]+2\frac{\partial}{\partial y}\left[(\nu+\nu_t)\frac{\partial v}{\partial y}\right]+g\beta(T-T_0) \tag{3}$$

$$\frac{\partial T}{\partial t}+u\frac{\partial T}{\partial x}+v\frac{\partial T}{\partial y}=\frac{\partial}{\partial x}\left[\left(\alpha_{air}+\frac{\nu_t}{Pr_t}\right)\frac{\partial T}{\partial x}\right]+\frac{\partial}{\partial y}\left[\left(\alpha_{air}+\frac{\nu_t}{Pr_t}\right)\frac{\partial T}{\partial y}\right] \tag{4}$$

$$\frac{\partial k}{\partial t}+u\frac{\partial k}{\partial x}+v\frac{\partial k}{\partial y}=\frac{\partial}{\partial x}\left[\left(\nu+\frac{\nu_t}{\sigma_k}\right)\frac{\partial k}{\partial x}\right]+\frac{\partial}{\partial y}\left[\left(\nu+\frac{\nu_t}{\sigma_k}\right)\frac{\partial k}{\partial y}\right]+P_k+G_k-\varepsilon \tag{5}$$

$$\frac{\partial \varepsilon}{\partial t}+u\frac{\partial \varepsilon}{\partial x}+v\frac{\partial \varepsilon}{\partial y}=\frac{\partial}{\partial x}\left[\left(\nu+\frac{\nu_t}{\sigma_\varepsilon}\right)\frac{\partial \varepsilon}{\partial x}\right]+\frac{\partial}{\partial y}\left[\left(\nu+\frac{\nu_t}{\sigma_\varepsilon}\right)\frac{\partial \varepsilon}{\partial y}\right]+\left(c_{1\varepsilon}(P_k+c_{3\varepsilon}G_k)-c_{2\varepsilon}\varepsilon\right)\frac{\varepsilon}{k} \tag{6}$$

inside the solid walls

$$\frac{\partial T}{\partial t}=\alpha_w\left(\frac{\partial^2 T}{\partial x^2}+\frac{\partial^2 T}{\partial y^2}\right) \tag{7}$$

The parameters c_μ, σ_k, $c_{1\varepsilon}$, $c_{2\varepsilon}$, $c_{3\varepsilon}$, σ_ε, Pr_t are constants that have the following empirical values (see Table 1).

The above governing Eqs. (1)–(7) are rewritten in another form excluding the pressure term. A transition is made from primitive variables "velocity–pressure" to non-primitive variables "stream function–vorticity".

The relations are given as

$$u=\frac{\partial \psi}{\partial y},\quad v=-\frac{\partial \psi}{\partial x},\quad \omega=\frac{\partial v}{\partial x}-\frac{\partial u}{\partial y}. \tag{8}$$

The complex energy transport phenomenon in a hollow block is solved in a dimensionless form. Reducing the system of differential Eqs. (1)–(7) to a dimensionless form makes it possible to better evaluate the results obtained. The scales of distance, time, temperature, velocity, stream function, kinetic energy of turbulence, dissipation rate of turbulence kinetic energy and vorticity are chosen as L, $\sqrt{g\beta\Delta T/L}$, $\Delta T=T_h-T_c$, $\sqrt{g\beta\Delta TL}$, $\sqrt{g\beta\Delta TL^3}$, $g\beta\Delta TL$, $\sqrt{g^3\beta^3(\Delta T)^3 L}$, $\sqrt{L/g\beta\Delta T}$, respectively.

Below are the additional restrictions for this formulation.

Initial restrictions are:

$\Psi(X,Y,0)=\Omega(X,Y,0)=K(X,Y,0)=E(X,Y,0)=\Theta(X,Y,0)=0$

Boundary conditions:

- at X = 0: $\Theta = 0.5$;
- at X = 1+2*h*/L: $\Theta = -0.5$;
- at Y = 0 and Y = 4+8*h*/L: $\partial\Theta/\partial Y=0$;
- at solid-air interfaces along X axis: $\Psi=0$, $\partial\Psi/\partial Y=0$, $\Theta_{air}=\Theta_w$, $\lambda_{w,air}\partial\Theta_w/\partial Y=\partial\Theta_{air}/\partial Y-N_{rad}Q_{rad}$;
- at solid-air interfaces along Y axis: $\Psi=0$, $\partial\Psi/\partial Y=0$, $\Theta_{air}=\Theta_w$, $\lambda_{w,air}\partial\Theta_w/\partial Y=\partial\Theta_{air}/\partial Y-N_{rad}Q_{rad}$.

Table 1. Turbulence model parameter values

Parameters	c_μ	$c_{1\varepsilon}$	$c_{2\varepsilon}$	$c_{3\varepsilon}$	σ_k	σ_ε	Pr_t
Values	0.09	1.44	1.92	0.8	1.0	1.3	1.0

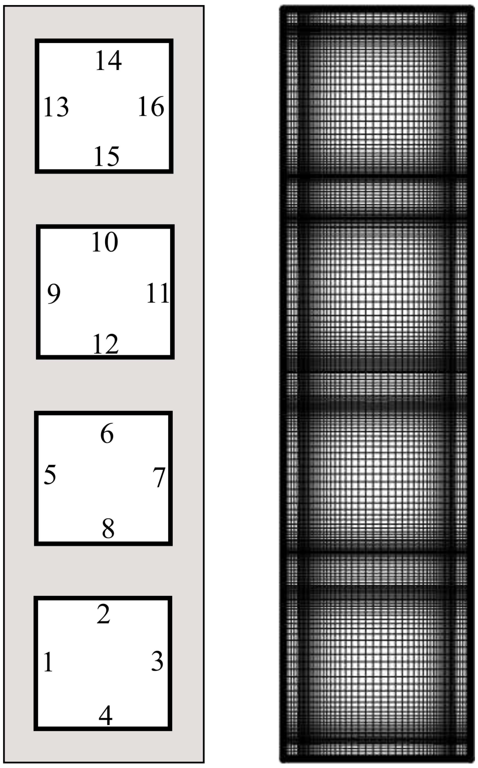

Fig. 2. Computational domain and utilized mesh

In order to investigate in detail the transport phenomena close to inner surfaces, a non-uniform grid is applied with special trigonometric transformation of coordinates:

$$\xi = a + \frac{b-a}{2}\left\{1 + \mathrm{tg}\left[\frac{\pi\kappa}{b-a}\left(X - \frac{a+b}{2}\right)\right] \Big/ \mathrm{tg}\left[\frac{\pi}{2}\kappa\right]\right\}, \tag{9}$$

$$\eta = a + \frac{b-a}{2}\left\{1 + \mathrm{tg}\left[\frac{\pi\kappa}{b-a}\left(Y - \frac{a+b}{2}\right)\right] \Big/ \mathrm{tg}\left[\frac{\pi}{2}\kappa\right]\right\}. \tag{10}$$

Here κ is a compaction factor and *a, b* are the shape factors. Computational domain and utilized mesh is shown in Fig. 2. The numbers from 1 to 16 indicate the corresponding surfaces for the convenience of demonstrating the average Nusselt numbers. The governing equations (1)–(7) with border restrictions are worked out employing the finite difference procedure [14].

First and second order derivatives for spatial coordinates have the form:

$$\frac{\partial\xi}{\partial X} = \frac{\pi\kappa}{2\cdot\mathrm{tg}\left\{\frac{\pi\kappa}{2}\right\}\cos^2\left\{\frac{\pi\kappa}{2}(2X-1)\right\}}, \quad \frac{\partial^2\xi}{\partial X^2} = \frac{(\pi\kappa)^2}{\mathrm{tg}\left\{\frac{\pi\kappa}{2}\right\}}\frac{\sin\left\{\frac{\pi\kappa}{2}(2X-1)\right\}}{\cos^3\left\{\frac{\pi\kappa}{2}(2X-1)\right\}}, \tag{11}$$

$$\frac{\partial\eta}{\partial Y} = \frac{\pi\kappa}{2\cdot\mathrm{tg}\left\{\frac{\pi\kappa}{2}\right\}\cos^2\left\{\frac{\pi\kappa}{2}(2Y-1)\right\}}, \quad \frac{\partial^2\eta}{\partial Y^2} = \frac{(\pi\kappa)^2}{\mathrm{tg}\left\{\frac{\pi\kappa}{2}\right\}}\frac{\sin\left\{\frac{\pi\kappa}{2}(2Y-1)\right\}}{\cos^3\left\{\frac{\pi\kappa}{2}(2Y-1)\right\}}. \tag{12}$$

The overall heat transfer through the inner vertical surfaces is determined by the mean convection and radiation Nusselt numbers. Thus, it is possible to estimate the contribution of radiation or convection to the ongoing thermal processes. In particular, the mean convection and radiation Nusselt numbers on the lower left vertical border are determined as:

$$Nu_{conv1} = \int_{h/L}^{1+h/L}\left|\frac{\partial\xi}{\partial X}\frac{\partial\Theta}{\partial\xi}\right|_{X=h/L} dY, \quad Nu_{rad1} = N_{rad}\int_{h/L}^{1+h/L}\left|Q_{rad}\right|_{X=h/L} dY. \tag{13}$$

A preliminary investigation of the influence of the grid spacing on the accuracy of the simulation results was carried out. Some results of this analysis are shown in Table 2. Based on the results obtained, we chose an average grid size of 120 × 480 elements for simulation analysis.

Table 2. Results of the grid independence study for $Ra = 10^8$, $\lambda_{w,air} = 27.27$

Grid size	Nu_{conv1}	% Change	Nu_{rad1}	% Change
60×240	9.85	–	6.11	–
120×480	7.28	26.09	5.77	5.56
180×720	7.06	3.02	5.65	2.07

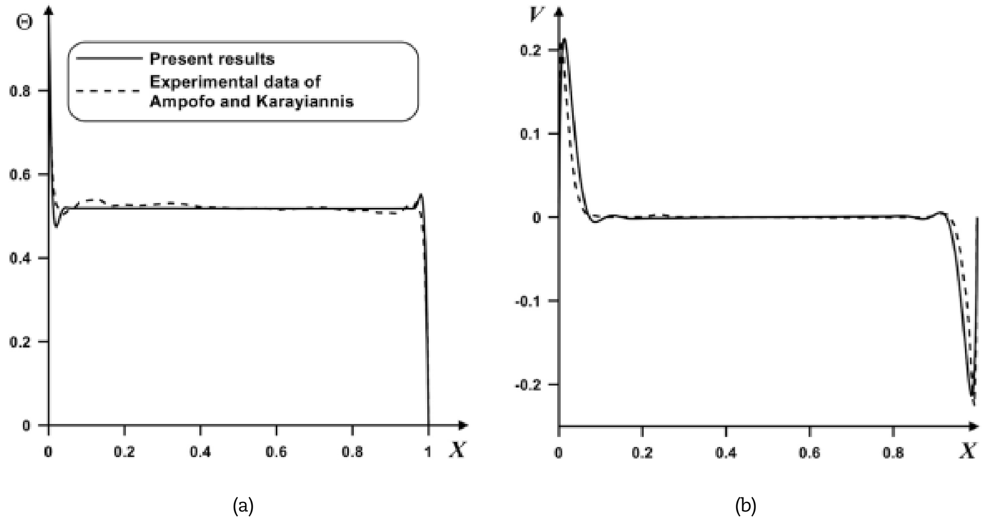

Fig. 3. The temperature patterns (a) and vertical velocity patterns (b) compared to experiments [32]

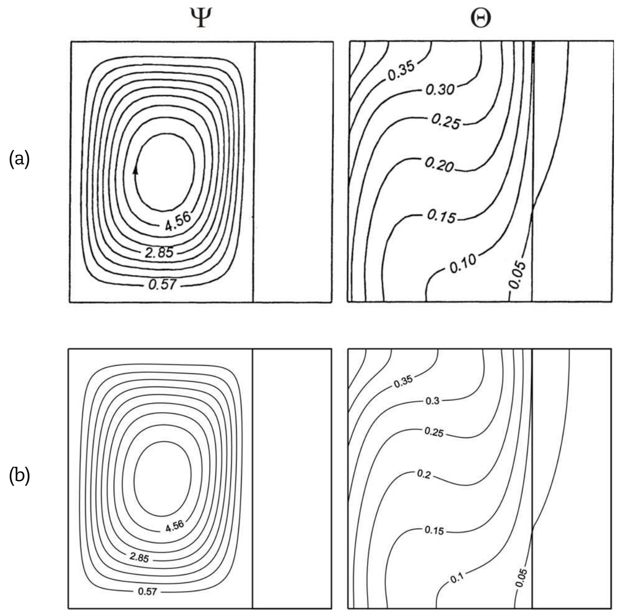

Fig. 4. Comparison of streamlines Ψ and isotherms Θ : a – numerical result of [33], b – present results

To assess the reliability of the numerical model, we performed simulations in accordance with the work [32]. A comparison of the temperature and vertical velocity profiles at mid-height of cavity is shown in Fig. 3.

As part of the verification of the numerical algorithm, the conjugate problem of convective heat transfer was solved. Figure 4 shows an agreement between the obtained isotherms and streamlines with the outcomes [33].

3. Results and Discussion

The results presented in this research are performed for the hollow block shown in Fig. 1. In this section, the effects of the surface emissivity of internal walls, Rayleigh number Ra and thermal conductivity of walls are discussed. The effect of these parameters on energy transport and airflow is insufficiently studied. The results for the average radiative Nu_{rad} and convective Nu_{conv} Nusselt numbers for different conditions are discussed. This section presents numerical results for $Ra = 10^7–10^8$, $\zeta = 0.897$, $Pr = 0.7$, $\lambda_{w,air} = 27.27–59.09$, $\tau = 10000$, $\tilde{\varepsilon} = 0 - 0.8$.

When modeling non-stationary modes of heat transfer, it is of great interest to analyze the evolution of energy transport and fluid circulation structures in time. Figure 5 shows the change in isotherms ⊠ with dimensionless time τ. At the initial moment of time, two convective cells are appeared inside the voids near the vertical walls. Their appearance is due to several factors, the main of which are the shape of the void and the boundary conditions of the problem. At $\tau = 20$, the merging of two hydrodynamic structures into one begins. Further growth of τ (see Fig. 5*b*) results in an appearance of one integral convective cell that determines the direction of flow in the voids in a clockwise direction.

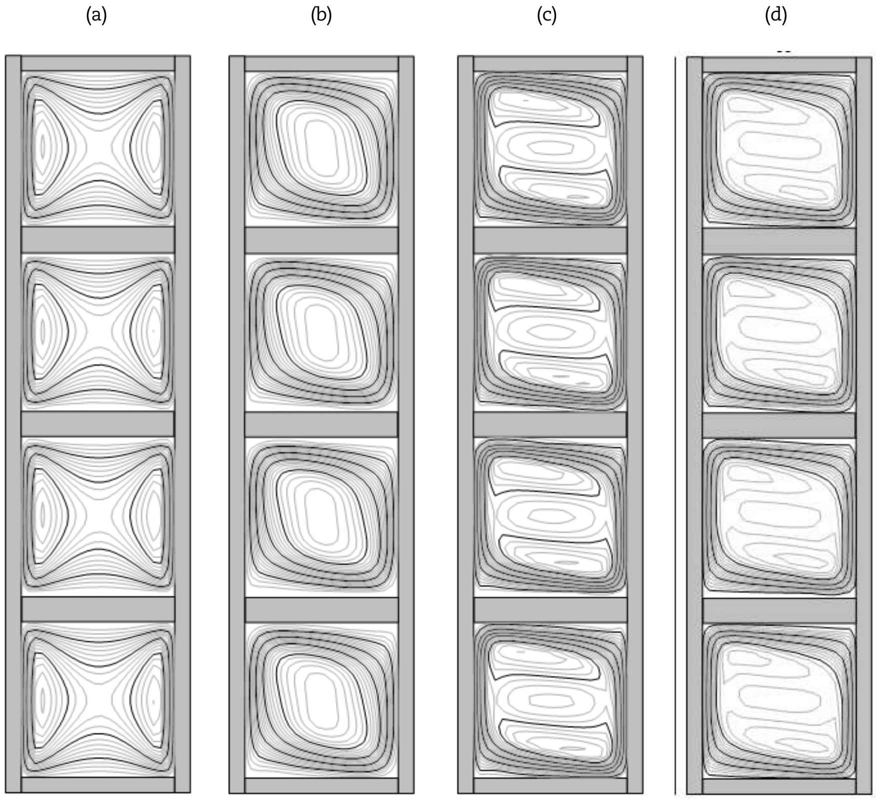

Fig. 5. Streamlines Ψ at $\tilde{\varepsilon} = 0.8$, $Ra = 10^7$: τ = 20 – a, τ = 100 – b, τ = 200 – c, τ = 500 – d

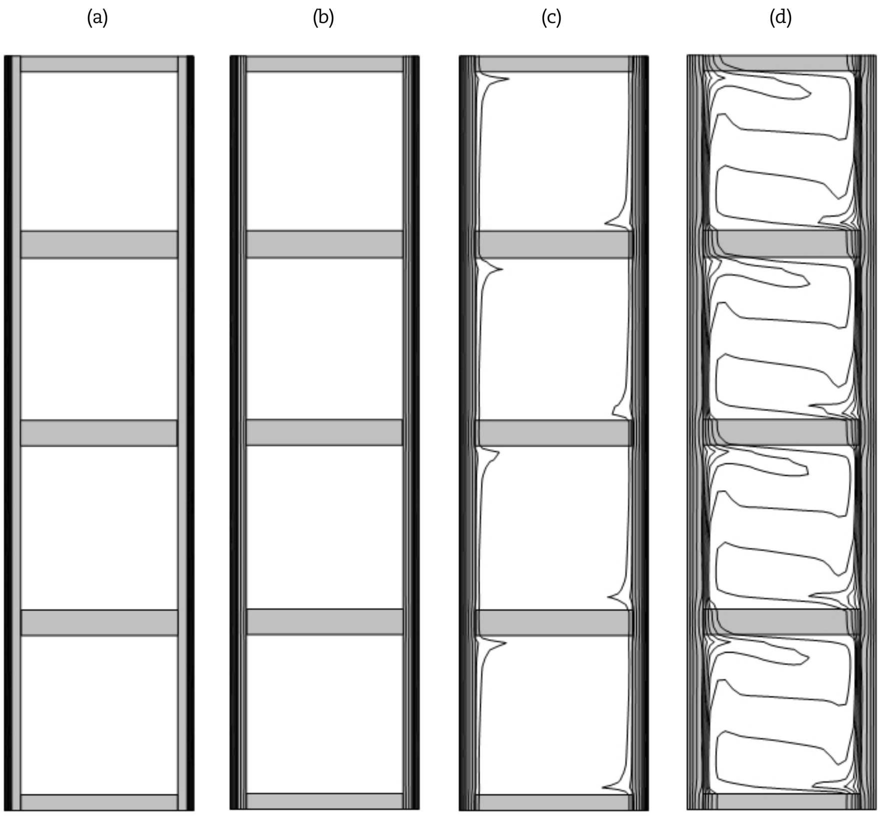

Fig. 6. Isotherms Θ at $Ra = 10^7$, $\tilde{\varepsilon} = 0.8$: τ = 20 – a, τ = 100 – b, τ = 200 – c, τ = 500 – d

The influence of τ on isotherms at $Ra = 10^7$ and $\tilde{\varepsilon} = 0.8$ is shown in Fig. 6. The main regime of energy transport at the initial moment of time (Fig. 6a and Fig. 6b) is the heat conduction. This is confirmed by the presence of vertically located isotherms inside solid walls. An increase in the dimensionless time causes intense penetration of temperatures from the external vertical walls. This leads to the appearance of a convective flow inside the hollow block.

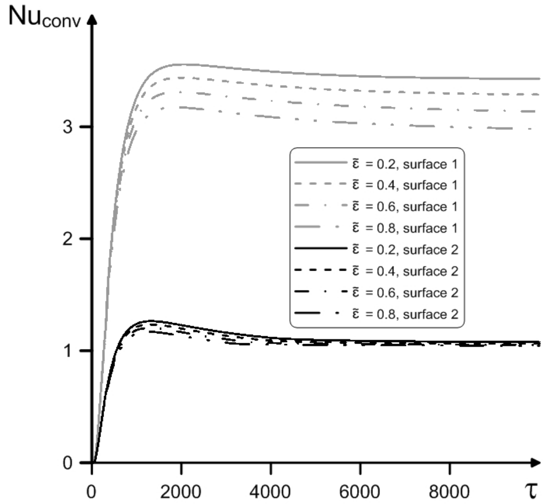

Fig. 7. Profiles of the mean convection *Nu* vs time and surface emissivity of internal walls at $Ra = 10^7$, $\lambda_{w,air} = 27.27$

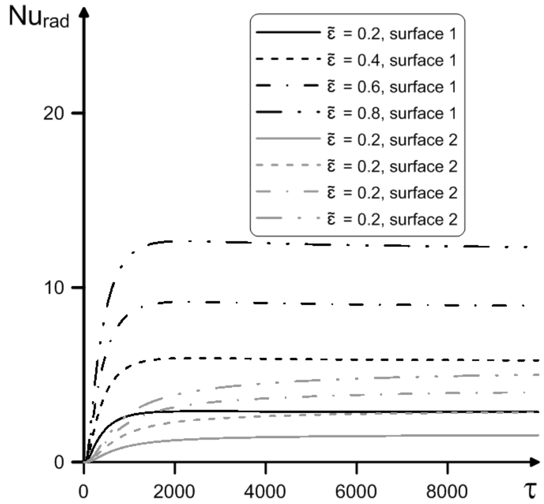

Fig. 8. Variation of the mean radiative *Nu* vs time and interface emissivity at $Ra = 10^7$, $\lambda_{w,air} = 27.27$

Comprehensive analysis of thermogravitational energy transport and thermal radiation provides a better understanding of the basic principles of energy transfer and fluid circulation in the hollow block. The profiles of the mean convection and radiation Nu as a function of the surface emissivity for $Ra = 10^7$, $\lambda_{w,air} = 27.27$ are presented in Figs. 7 and 8. In this work, when performing the calculations of free convection with surface radiation heat transfer, surfaces are diffuse and gray. The phenomenon of heat transfer between these walls (due to multiple reflection and absorption) is complicated in comparison with a similar process for absolutely black bodies. If, in the general case, the surface emissivity of the body depends on the wavelength, angle, and temperature of the body, then for the case of diffuse and gray surfaces, the surface emissivity and absorbance depend only on temperature.

A raise of the surface emissivity of inner borders results in an insignificant decrease in convective heat transfer. In particular, at $\tau = 10000$ surface emissivity reduces the mean convective Nu on surface 1 up to 13 % for range of $\tilde{\varepsilon}$ between 0.2 and 0.8. So, an increment of the surface emissivity results in a decrease in the rate of convective energy transport in the voids of the block. This fact can be illustrated by the typical reduction of the maximum values of the stream function:

$$\left|\Psi\right|_{\max}^{\tilde{\varepsilon}=0.2} = 0.0243 > \left|\Psi\right|_{\max}^{\tilde{\varepsilon}=0.6} = 0.0237 > \left|\Psi\right|_{\max}^{\tilde{\varepsilon}=0.8} = 0.0233. \quad (14)$$

A rise of the mean radiative Nu on surface 1 with growing $\tilde{\varepsilon}$ has been found. At $\tau = 10000$, a raise of surface emissivity values from 0.2 to 0.8 results in an increase in of Nu_{rad} up to 4.31 times. In this connection, the use of hollow building element with a low emissivity of internal surfaces will significantly reduce the energy consumption of buildings.

To analyze the impact of surface radiation on energy transport, it is also necessary to investigate the mean integral heat transfer coefficients on other surfaces. Variations of various parameters (maximum absolute magnitude of the stream function, mean convective Nu and mean radiative Nu) for $Ra = 10^7$, $\lambda_{w,air} = 27.27$ and $\tau = 10000$ are shown in Table 3. The values presented in Table 3 confirm that a growth of the values of the emissivity of interfaces results in two oppositely directed effects. The first effect is an essential augmentation of the radiative Nu. The second one is in a slight decrease in the intensity of convective energy transport. In order to improve the thermal insulation properties of a hollow building element, it is advisable to reduce the interface emissivity. This is possible, for example, by reducing the roughness of the inner walls. The radiation contribution has an order similar to that of free convection. In this connection, radiative heat transfer in hollow blocks must be calculated with adequate accuracy.

As a material for a hollow building element, brick and concrete were considered with thermal conductivity coefficients 0.6 W/(m·K) and 1.3 W/(m·K), respectively. In Figs. 9 and 10, variations of mean convective and radiative *Nu* on surface 4 are demonstrated. Mean *Nu* are increased with a growth of the heat conductivity ratio. At $\tau = 10000$ and $\tilde{\varepsilon} = 0.8$, Nu_{rad} is increased up to 9% for a range of $\lambda_{w,air}$ between 27.27 and 59.09. This is due to a reduction of thermal resistance of the walls of the hollow block. Such behavior results in an increase in of the temperature difference on opposite walls, which in turn results in an enhancement of convective and radiative energy transport.

Table 3. Variations of different considered parameters for $\tau = 10000$, $Ra = 10^7$ and $\lambda_{w,air} = 27.27$

Surface number	Surface emissivity	$\left|\Psi\right|_{\max}$ for whole block	Nu_{conv}	Nu_{rad}
5	0.2	0.0243	2.73	2.66
	0.4	0.0240	2.66	5.46
6	0.2	0.0243	1.09	1.44
	0.4	0.0240	1.07	2.66
9	0.2	0.0243	2.72	2.65
	0.4	0.0240	2.65	5.45
10	0.2	0.0243	1.09	1.44
	0.4	0.0240	1.07	2.66

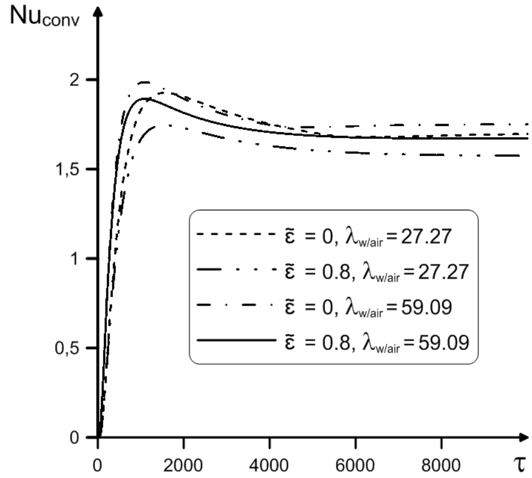

Fig. 9. Variation of the average convective Nusselt number at surface 4 vs time and heat conductivity ratio of walls at $Ra = 10^7$

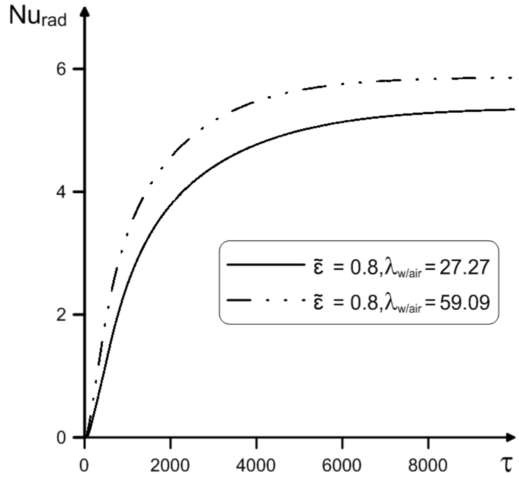

Fig. 10. Variation of Nu_{rad} at surface 4 vs time and thermal conductivity ratio of walls at $Ra = 10^7$

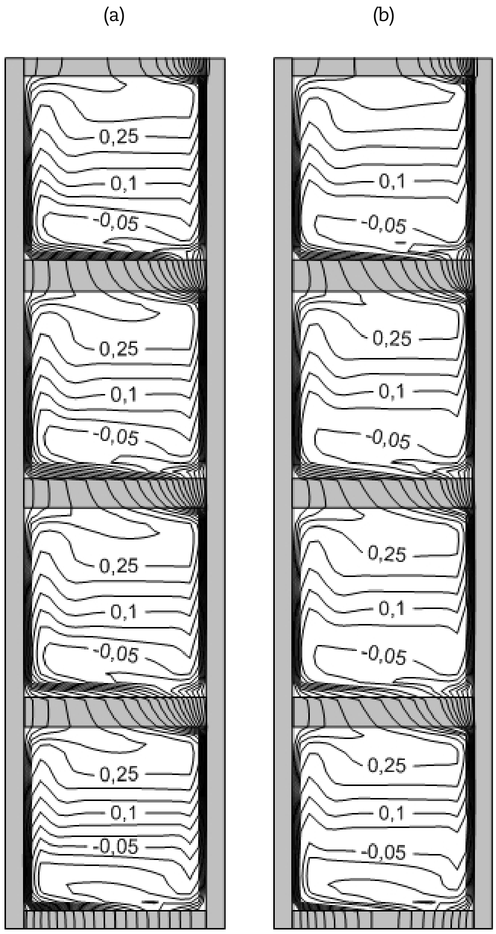

Fig. 11. Isotherms Θ for $Ra = 10^7$, $\lambda_{w,air} = 27.27 : \tilde{\varepsilon} = 0 - a$, $\tilde{\varepsilon} = 0.8 - b$

Figure 11 illustrates the variation of isotherms Θ with surface emissivity values. Regardless of whether the radiation component of the energy transfer is taken into account, a thermal boundary layer is appeared near the inner vertical surfaces. This is visually reflected in the thickening of isotherms near these surfaces. It can be also seen that distribution of isotherms in the voids is changed insignificantly. At the same time, the average temperature of a hollow block decreases by 4-4.5% (at different Rayleigh numbers) with an increase in emissivity from 0 to 0.8.

Table 4 shows change of mean convective Nu at $\tau = 10000$, $\lambda_{w,air} = 27.27$, $\tilde{\varepsilon} = 0$. The Rayleigh number is a non-dimensional factor that defines the nature of a liquid circulation under the impact of a temperature drop. Growth of the Rayleigh number can occur due to an increase in the characteristic size of the enclosure or due to a raise of the thermal drop. As it is shown, a raise of Ra has no essential impact on the flow nature, except for a slight increase in the intensity of convective flow.

Table 4. Average convective Nusselt numbers at τ = 10000, $\lambda_{w,air}$ = 27.27, $\tilde{\varepsilon} = 0$

Rayleigh number	Nu_{conv} on surface 1	Nu_{conv} on surface 6	Nu_{conv} on surface 15
10^7	3.561	1.111	2.433
$5{\cdot}10^7$	6.209	1.650	3.649
10^8	7.755	1.947	4.241

4. Conclusions

Computational investigation of complex energy transport by conduction, thermal convection and surface radiation through a hollow block has been carried out. Based on the finite difference procedure, the mathematical model was developed to study the impact of the interface emissivity, Rayleigh number and thermal conductivity of solid walls on the overall energy transport through the hollow block. Numerical simulation is carried out using the calculation code written by mean of C++ programming language. In order to thicken the calculated mesh to the interfaces, a special trigonometric transformation of coordinates was applied. Distributions of integral (integral heat transfer coefficients) and scalar (stream function and temperature profiles) parameters are obtained. A raise of *Ra* results in a significant increment of the intensity of energy transport due to both mechanisms of thermal convection and radiation. Reducing the interface emissivity results in two oppositely directed effects. There is a significant decrease in the mean radiative *Nu* and a slight rise of Nu_{conv}. Therefore, the use of materials with low emissivity values for the internal surfaces of hollow blocks as a building material will greatly help to reduce the energy consumption in buildings.

Author Contributions

I.V. Miroshnichenko and M.A. Sheremet conceived the main concept. All authors contributed to the investigation and data analysis. I.V. Miroshnichenko wrote the manuscript. All authors contributed to the writing of the final manuscript. All authors have read and agreed to the published version of the manuscript.

Acknowledgments

This work was supported by the Tomsk State University Development Programme (Priority-2030).

Conflict of Interest

The authors declared no potential conflicts of interest concerning the research, authorship, and publication of this article.

Funding

Not Applicable.

Data Availability Statements

Not Applicable.

Nomenclature

F_{k-i}	View factor between *k*-th and *i*-th elements of a chamber
L	Void size (m)
g	Gravity acceleration (m/s^2)
$\tilde{h}$	Thermally transport factor (W/m^{2}K)
k	Turbulence kinetic energy (m^2/s^2)
h	Walls thickness (m)
K	Dimensionless turbulent kinetic energy
$G_k = -\dfrac{\nu_t}{\Pr_t}\dfrac{\partial T}{\partial y}$	Generation/destruction of buoyancy turbulent kinetic energy
E	Dimensionless dissipation rate of turbulent kinetic energy
$Ra = g\beta(T_h - T_c)L^3/\nu\alpha_{air}$	Rayleigh number
Nu_{con}	Mean convective Nusselt number
$N_{rad} = \sigma T_h^4 L/[\lambda_{air}(T_h - T_c)]$	Radiation number
$\Pr = \nu/\alpha_{air}$	Prandtl number
Nu_{rad}	Mean radiative Nusselt number
$P_k = \nu_t\left[2\left(\dfrac{\partial u}{\partial x}\right)^2 + 2\left(\dfrac{\partial v}{\partial y}\right)^2 + \left(\dfrac{\partial u}{\partial y} + \dfrac{\partial v}{\partial x}\right)^2\right]$	Shearing generation
$\Pr_t = \nu_t/\alpha_t$	Turbulent Prandtl number
R_k	Dimensionless radiosity of the *k*-th element of a chamber
Q_{rad}	Dimensionless net radiative thermal flux
T_h	Temperature on the left wall (K)

t	Dimensional time (s)
T_c	Temperature on the right wall (K)
T	Dimensional temperature (K)
Θ_f	Dimensionless temperature of fluid
Θ	Dimensionless temperature
u, v	Velocity projections for x and y axis (m/s)
U, V	Dimensionless velocity projections for X and Y axis
Θ_w	Dimensionless temperature of wall
X, Y	Dimensionless Cartesian coordinates
ε	Dissipation rate of turbulent kinetic energy (m^2/s^3)
$\zeta = T_c/T_h$	Temperature parameter
β	Factor of volumetric heat expansion (1/K)
α_w	Heat diffusivity of the wall material (m^2/s)
α_{air}	Air heat diffusivity (m^2/s)
$\alpha_{i,j} = \alpha_i/\alpha_j$	Heat diffusivity ratio
$\tilde{\varepsilon}$	Surface emissivity of wall surfaces
λ_{air}	Air heat conductivity (W/mK)
λ_w	Heat conductivity of the wall material (W/mK)
$\lambda_{i,j} = \lambda_i/\lambda_j$	Heat conductivity ratio
ν	Kinematic viscosity (m^2/s)
ψ	Stream function (m^2/s)
ω	Vorticity (s^{-1})
$\nu_t = c_\mu k^2/\varepsilon$	Turbulent viscosity (m^2/s)
Ψ	Dimensionless stream function
ξ, η	Non-dimensional variables
Ω	Dimensionless vorticity
τ	Dimensionless time
σ	Stefan–Boltzmann constant (W/m^2K^4)

References

[1] Stazizar, A.J., Investigation of Flow Phenomena in a transonic Fan Rotor Using Laser Anemometry, *ASME Journal of Engineering for Gas Turbines and Power*, 107(2), 1985, 427-435.
[2] Myers, R.H., Montgomery, D.C., *Response Surface Methodology: Process and product optimization using designed experiments*, John Wiley & Sons, New York, 1995.
[3] Guinta, A.A., *Aircraft Multidisciplinary Design Optimization Using Design of Experimental Theory and Response Surface Modeling Methods*, Ph.D. Thesis, Department of Aerospace Engineering, Virginia Polytechnic Institute and State University, Blacksburg, VA, 1997.
[4] Jameson, A., Schmidt, W., Turkel, E., Numerical Solutions of the Euler Equation by Finite Volume Methods Using Runge-Kutta Time Stepping Schemes, *AIAA Journal*, 81, 1981, 1259.
[5] Denton, J.D., Xu, L., The Effects of Lean and Sweep on Transonic Fan Performance, *ASME Turbo Expo*, Amsterdam, Netherlands, GT-2002-30327, 2002.
[6] Burns, T., US Patent No. 358498, 1995.
[1] Miroshnichenko, I.V., Sheremet, M.A., Turbulent natural convection heat transfer in rectangular enclosures using experimental and numerical approaches: A review, *Renewable and Sustainable Energy Reviews*, 82, 2018, 40–59.
[2] Patil, S., Sharma, A.K., Velusamy, K., Conjugate laminar natural convection and surface radiation in enclosures: Effects of protrusion shape and position, *International Communications in Heat and Mass Transfer*, 76, 2016, 139–146.
[3] Altac, Z., Ugurlubilek, N., Assessment of turbulence models in natural convection from two- and three-dimensional rectangular enclosures, *International Journal of Thermal Sciences,* 107, 2016, 237–246.
[4] Ben-Nakhi, A., Mahmoud, M.A., Conjugate turbulent natural convection in the roof enclosure of a heavy construction building during winter, *Applied Thermal Engineering*, 28, 2008, 1522–1535.
[5] Sharma, A.K., Velusamy, K., Balaji, C., Turbulent natural convection in an enclosure with localized heating from below, *International Journal of Thermal Sciences*, 46, 2007, 1232–1241.
[6] Martyushev, S.G., Miroshnichenko, I.V., Sheremet, M.A., Numerical analysis of spatial unsteady regimes of conjugate convective-radiative heat transfer in a closed volume with an energy source, *Journal of Engineering Physics and Thermophysics*, 87, 2014, 124–134.
[7] Miroshnichenko, I., Sheremet, M., Chamkha, A.J., Turbulent natural convection combined with surface thermal radiation in a square cavity with local heater, *International Journal of Numerical Methods for Heat and Fluid Flow*, 28(7), 2018, 1698–1715.
[8] Ibrahim, A., Saury, D., Lemonnier, D., Coupling of turbulent natural convection with radiation in an air-filled differentially-heated cavity at Ra = 1.5×10^9, *Computers and Fluids*, 88, 2013, 115–125.
[9] Abouricha, N., El Alami, M., Gounni, A., Lattice Boltzmann modeling of natural convection in a large-scale cavity heated from below by a centered source, *Journal of Heat Transfer*, 141, 2019, 062501.
[10] Dixit, H.N., Babu, V., Simulation of high Rayleigh number natural convection in a square cavity using the lattice Boltzmann method, *International Journal of Heat and Mass Transfer*, 49, 2006, 727–739.
[11] Shi, Y., Zhao, T.S., Guo, Z.L., Finite difference-based lattice Boltzmann simulation of natural convection heat transfer in a horizontal concentric annulus, *Computers and Fluids*, 35, 2006, 1–15.
[12] Gibanov, N.S., Sheremet, M.A., Numerical investigation of conjugate natural convection in a cavity with a local heater by the lattice Boltzmann method, *Fluids*, 6(9), 2021, 316.
[13] Zhou, L., Liu, J., Huang, Q., Wang, Y., Analysis of combined natural convection and radiation heat transfer in a partitioned rectangular enclosure with semitransparent walls, *Transactions of Tianjin University*, 25, 2019, 472–487.
[14] Miroshnichenko, I.V., Sheremet, M.A., Numerical simulation of turbulent natural convection combined with surface thermal radiation in a square cavity, *International Journal of Numerical Methods for Heat & Fluid Flow*, 25, 2015, 1600–1618.
[15] Lari, K., Baneshi, M., Nassab, S.A.G., Komiya, A., Maruyama, S., Combined heat transfer of radiation and natural convection in a square cavity containing participating gases, *International Journal of Heat and Mass Transfer*, 54, 2011, 5087–5099.
[16] Boukendil, M., Abdelbaki, A., Zrikem, Z., Detailed numerical simulation of coupled heat transfer by conduction, natural convection and radiation through double honeycomb walls, *Building Simulation*, 5, 2012, 337–344.
[17] Boukendil, M., Abdelbaki, A., Zrikem, Z., Numerical simulation of coupled heat transfer through double hollow brick walls: Effects of mortar joint

thickness and emissivity, *Applied Thermal Engineering*, 125, 2017, 1228–1238.
[18] Jamal, B., Boukendil, M., El Moutaouakil, L., Abdelbaki, A., Zrikem, Z. Thermal analysis of hollow clay bricks submitted to a sinusoidal heating, *Materials Today: Proceedings*, 45, 2021, 7399–7403.
[19] Alhazmy, M.M., Internal baffles to reduce the natural convection in the voids of hollow blocks, *Building Simulation*, 3, 2010, 125–137.
[20] Waqas, H., Farooq, U., Hussain, M., Alanazi, A.K., Brahmia, A., Hammouch, Z., Cattaneo-Christov heat and mass flux effect on upper-convected Maxwell nanofluid with gyrotactic motile microorganisms over a porous sheet, *Sustainable Energy Technologies and Assessments*, 52, 2022, 102037.
[21] ul Haq, M.R., Hussain, M., Bibi, N., Shigidi, I.M., Pashameah, R.A., Alzahrani, E., Energy transport analysis of the magnetized forced flow of power-law nanofluid over a horizontal wall, *Journal of Magnetism and Magnetic Materials*, 560, 2022, 169681.
[22] do Carmo Zidan, D., Maia, C.B., Safaei, M.R., Performance evaluation of various nanofluids for parabolic trough collectors, *Sustainable Energy Technologies and Assessments*, 50, 2022, 101865.
[22] Imran, M., Farooq, U., Waqas, H., Anqi, A.E., Safaei, M.R., Numerical performance of thermal conductivity in Bioconvection flow of cross nanofluid containing swimming microorganisms over a cylinder with melting phenomenon, *Case Studies in Thermal Engineering*, 26, 2021, 101181.
[23] Alazwari, M.A., Safaei, M.R., Combination effect of baffle arrangement and hybrid nanofluid on thermal performance of a shell and tube heat exchanger using 3-D homogeneous mixture model, *Mathematics*, 9(8), 2021, 881.
[24] Abu-Hamdeh, N.H., Alsulami, R.A., Rawa, M.J., Alazwari, M.A., Goodarzi, M., Safaei, M.R., A Significant Solar Energy Note on Powell-Eyring Nanofluid with Thermal Jump Conditions: Implementing CattaneoChristov Heat Flux Model, *Mathematics*, 9(21), 2021, 2669.
[25] Abu-Hamdeh, N.H., Aljinaidi, A.A., Eltaher, M.A., Almitani, K.H., Alnefaie, K.A., Abusorrah, A.M., Implicit Finite Difference Simulation of Prandtl-Eyring Nanofluid over a Flat Plate with Variable Thermal Conductivity: A Tiwari and Das Model, *Mathematics*, 9(24), 2021, 3153.
[26] Barman, T., Roy, S., Chamkha, A.J., Magnetized Bi-convective Nanofluid Flow and Entropy Production Using Temperature-sensitive Base Fluid Properties: A Unique Approach, *Journal of Applied and Computational Mechanics*, 8(4), 2022, 1163-1175.
[27] Manjunatha, S., Puneeth, V., Gireesha, B.J., Chamkha, A.J., Theoretical Study of Convective Heat Transfer in Ternary Nanofluid Flowing past a Stretching Sheet, *Journal of Applied and Computational Mechanics*, 8(4), 2022, 1279-1286.
[28] Alazwari, M.A., Algarni, M., Safaei, M.R., Effects of various types of nanomaterials on PCM melting process in a thermal energy storage system for solar cooling application using CFD and MCMC methods, *International Journal of Heat and Mass Transfer*, 195, 2022, 123204.
[29] El Moutaouakil, L., Zrikem, Z., Abdelbaki, A., Interaction of surface radiation with laminar and turbulent natural convection in tall vertical cavities: analysis and heat transfer correlations, *Heat Transfer Engineering*, 36, 2015, 1472–1484.
[30] Mikhailenko, S.A., Miroshnichenko, I.V., Sheremet, M.A., Thermal radiation and natural convection in a large-scale enclosure heated from below: Building application, *Building Simulation*, 14, 2021, 681–691.
[31] Kogawa, T., Okajima, J., Sakurai, A., Komiya, A., Maruyama, S., Influence of radiation effect on turbulent natural convection in cubic cavity at normal temperature atmospheric gas, *International Journal of Heat and Mass Transfer*, 104, 2017, 456–466.
[32] Ampofo, F., Karayiannis, T.G., Experimental benchmark data for turbulent natural convection in an air filled square cavity, *International Journal of Heat and Mass Transfer*, 46, 2003, 3551–3572.
[33] Ben Yedder, R., Bilgen, E., Turbulent natural convection and conduction in enclosures bounded by a massive wall, *International Journal of Heat and Mass Transfer*, 38, 1995, 1879–1891.

ORCID iD

Igor V. Miroshnichenko https://orcid.org/0000-0002-8582-3326
Mikhail A. Sheremet https://orcid.org/0000-0002-4750-0227

How to cite this article: Miroshnichenko I.V., Sheremet M.A. Influence of Thermal Radiation on Heat Transfer through a Hollow Block, *J. Appl. Comput. Mech.*, 9(2), 2023, 419–429. https://doi.org/10.22055/jacm.2022.41759.3805